

iScience, Volume 26

Supplemental information

**Seizure enhances SUMOylation
and zinc-finger transcriptional repression
in neuronal nuclei**

Hui Rong Soon, Jessica Ruth Gaunt, Vibhavari Aysha Bansal, Clara Lenherr, Siu Kwan Sze, and Toh Hean Ch'ng

SUPPLEMENTAL FIGURES AND LEGENDS

Figure S1: CaMKII α -Cre::SUN1-sfGFP expression in excitatory neurons (related to Figure 1A). Representative images of the CA1 pyramidal layer and DG of the hippocampus, and the cortex of a 4-week-old CaMKII α -Cre::SUN1-sfGFP mouse. Sections were immunolabelled with antibodies against GAD67 to identify inhibitory neurons (white arrowheads). SUN1-sfGFP expression in excitatory neurons does not overlap with GAD67-positive inhibitory neurons in any of the brain regions. Hoechst (blue); GAD67 (red); SUN1-sfGFP (green); Scale bar, 10 μ m.

Figure S2: pCREB (S133) expression is elevated in the cortex (related to Figure 1E-F). Representative images of brain sections showing elevated pCREB (S133) expression in cortex of pilocarpine-injected mouse. Brain sections from 4-week-old mice were either mock- or pilocarpine- injected to induce seizures and immunolabelled with antibodies to detect pCREB (S133). SUN1-GFP (green); Hoechst (blue); pCREB (S133) (red). Scale bars, 100 μ m; 20 μ m (magnified).

Figure S3: INTACT isolation of nuclei at the interface stage (related to Figure 1G). Confocal images of nuclei isolated from the iodixanol gradient interface from ultracentrifugation before and after immunopurification. Mixed populations of nuclei are detected at the interface while immunopurified SUN1-sfGFP nuclei were largely bound to anti-GFP antibody coated beads. Scale bar, 50 μ m; 20 μ m (magnified). Hoechst (blue); SUN1-sfGFP (green).

Figure S4: INTACT nuclear purification efficiency (related to Figure 1G). Average yield and specificity of the isolated nuclei at the interface stage and after immunopurification with anti-GFP antibodies.

Figure S5: TMT6-labeled MS/MS VSN normalization (related to Figure 2A-B). Graph plotted from NormalyzerDE showing the reduction in pooled coefficient of variance (pooled-CV) after variance stabilizing normalisation (VSN) as compared to other normalisation methodologies.

Figure S6: STRING network of seizure-depleted nuclear proteins (related to Figure 2C). STRING network for seizure-depleted nuclear proteins (N=195; Interaction score > 0.7 with disconnected nodes hidden from network). Selected GO clusters that correspond to Figure 2D enrichment score plots are highlighted in the network.

Figure S7: Flowchart of nuclear extraction (related to Figure 3). Flow diagram for the nuclear isolation from mouse forebrain for western blots

Figure S8: AP1 complex expression during seizures in hippocampal neurons (related to Figure 3A-B). Seizure- and Bic-induced AP bursting enhances accumulation of AP-1 complex subunits in neuronal nuclei. (A) Representative images of dentate gyrus (DG), CA1 and CA3 of the hippocampus, and piriform cortex (PIR) of mock- and pilocarpine-injected animals immunolabelled with anti-FOS antibodies. SUN1-GFP (green); Hoechst (blue); FOS (red); Scale bars, 10 μ m. (B) Percent change in nuclear intensity for FOS.

Nuclear intensities for FOS were measured by random selection of SUN1-sfGFP-positive nuclei demarcated by Hoechst nuclear stain. All quantifications are normalised to mean nuclear intensity from mock-injected animals (N=3 pairs of animals; n=75 cells quantified across sections). (C) Hippocampal neurons (DIV14 to 15) were stimulated with Bic (40 μ M), a pro-convulsant drug, for 30 min before washed, fixed and immunostained with antibodies against FOS (red); Hoechst (blue) and MAP2 (cyan). Scale bars, 5 μ m. (D) Quantification of hippocampal neurons in basal condition or stimulated with Bic. Values were derived by normalising against mean nuclear intensity for each independent experiment (N=3 independent experiments, n=60 total number of cells quantified across experiments). (E) Representative images of dentate gyrus (DG), CA1 and CA3 of the hippocampus, and piriform cortex (PIR) of mock- and pilocarpine-injected animals immunolabelled with anti-JUNB antibodies. SUN1-GFP (green); Hoechst (blue); JUNB (red); Scale bars, 10 μ m. (F) Quantification of JUNB in SUN1-sfGFP-positive nuclei as outlined in (B) (N=3 pairs of animals; n=75 cells quantified across sections). (G) Hippocampal neurons (DIV14 to 15) were stimulated with Bic (40 μ M) as described in (C). JUNB (red); Hoechst (blue); MAP2 (cyan); Scale bars, 5 μ m. (H) Quantification of hippocampal neurons similar as described in (D) (N=3 independent experiments, n=60 total number of cells quantified across experiments). All statistics were performed using Mann-Whitney test with plots showing means \pm SEM, $p < 0.05$ (*), $p < 0.0001$ (****).

Figure S9: Nuclear localization of SUMO-1 and SUMO-2/3 in neuronal nuclei (related to Figure 4A and 4F). Confocal micrographs of brain sections, focusing on CA1 pyramidal cell layer showing immunohistochemistry of SUMO-1 and SUMO-2/3 signal intensity and corresponding lookup tables (LUTs; far right panels for each row). Red circles denote outline of excitatory neuronal nuclei as determined by SUN1-GFP intensities. Scale bars, 10 μ m.

Figure S10: Cytoplasmic SUMO-2/3 after Bic stimulation (related to Figure 4C). Experiments are performed exactly as described in Figure 5C. Hippocampal neurons (DIV14-15) were stimulated with bicuculline (Bic; 40 μ M) for 30 min and 24 h. After stimulation, neurons were fixed and immunostained with anti-SUMO-2/3 antibodies. To detect the much lower cytoplasmic signal, the intensity for each image is uniformly increased, resulting in oversaturation of signal in the nucleus (white). Images are shown as LUTs and Scale bars, 5 μ m. Cytoplasmic intensities were measured, and all experimental values were normalized against mean cytoplasmic intensity at basal state (N=3 independent experiments; n=60 total number of cells quantified across all conditions). All statistics were performed using Mann-Whitney test with bar plots showing means \pm SEM, < 0.0001 (****).

Figure S11: Distribution of expressed transcript groups (related to Figure 5A). The different subtypes of transcripts detected by RNA-seq are listed as a fraction of the total RNA population in the pie chart. The majority of sequenced transcripts belong to protein-coding transcripts (89.05%).

Figure S12: Expression of known activity-regulated genes (related to Figure 5A-C). Overlay of previously characterised, temporally defined, subclasses of activity-dependent transcripts on volcano plot of the seizure transcriptome ¹⁴⁵.

Figure S13: Upregulation of *Fos* and *JunB* gene expression in seizing animals by PSR (related to Figure 5G). qPCR of *Fos* and *Junb* (N=5 mock v. pilocarpine injected animals). Relative gene expression levels were determined by normalising to average Δ Ct values for all mock-injected animals. All statistics were performed using one-sample t-test with plots showing means \pm SEM, $p < 0.05$ (*), $p < 0.01$ (**).

Figure S14: THAP11 bipartite DNA binding motif (related to Figure 5H). Position weight matrix for THAP11-binding motif and histogram of binding site locations relative to the transcription start site (TSS) for genes with maximum binding scores above background average.

Figure S15: Kainic acid-induced seizures downregulate KRAB-ZFP gene expression (related to Figure 5E-F). GSEA plots showing enrichment of KRAB genes in hippocampal neuronal nuclei at 1 h, 6 h and 48 h post-induction of kainic acid-induced seizure ⁵⁴.

Figure S16: Exposure of rodents to a novel environment drives activity-dependent suppression of KRAB-ZFP gene expression and altered chromatin accessibility (related to Figure 5E-F). GSEA plots showing enrichment of KRAB genes in (i) single-nucleus RNA-seq of Fos-positive versus Fos-negative dentate granule cells 1 h following 15 min novel environment exploration ⁵⁵ and (ii) Assay for Transposase-Accessible Chromatin sequencing (ATAC-seq) of sorted Fos-positive hippocampal neuronal nuclei versus Fos-negative nuclei following 1 h novelty exploration ⁵⁴.

Figure S17: THAP11 is localized in neuronal nuclei but is unaltered by bicuculline (related to Figure 5G-I). (A) High resolution Airyscan confocal images of a hippocampal neuron (DIV14) labelled with THAP11 (red), MAP2 (cyan) and Hoechst (blue). Scale bar at 10 μ m. (B) Bic treatment of cultured neurons (DIV 21; 40 μ M; 30 min) before cells were fixed, labelled, and quantified for THAP11 (n=16 Basal; n=19 Bic, Mann-Whitney with plots showing means \pm SEM). Experiment was replicated two more times in DIV 14 and DIV 28 neurons, each with similar results. (C) Western blot of hippocampal neuronal lysates (DIV 21) either mock or Bic (40 μ M) stimulated for 30 min. THAP11 protein band was normalized against GAPDH, quantified (N=3) and analysed with paired t-test. Plots reported as \pm SEM. (D) Transcriptome values including Log₂FC for top Pscan targets. (E) Conserved SUMO motif in THAP11 across species.

Figure S18: GSEA profiles of methylation and DNA repair in nuclear proteome and transcriptome (related to Figure 7). GSEA plots for methylation (GO:0032259) and DNA repair (GO:0006281) in nuclear proteome and transcriptome during seizures.

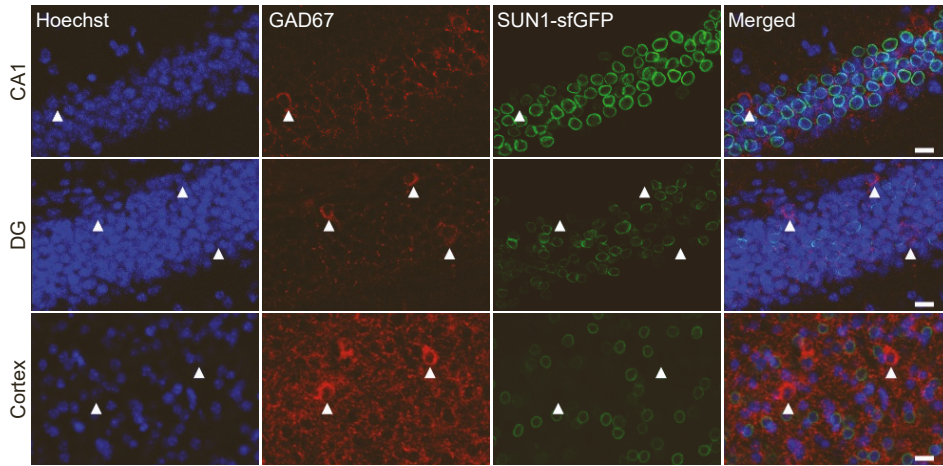
Figure S19: GSEA profiles of transcriptional repression (related to Figure 7). GSEA plots indicate increased nuclear expression of transcriptional or translational repressors (UniProt keyword KW-0678) in the proteome and transcriptome during seizure.

Figure S20: Coverage of introns and exons across genebody for transcripts of varying length (related to Figure 6A-C). Coverage plots for exonic and intronic regions of protein-coding genes generated using superintronic¹¹². Mean coverage plots for all samples and non-overlapping genes. Genes are divided into equal groups of short, medium, and long transcripts, and gene bodies are divided into 20 bins from 5' to 3' end.

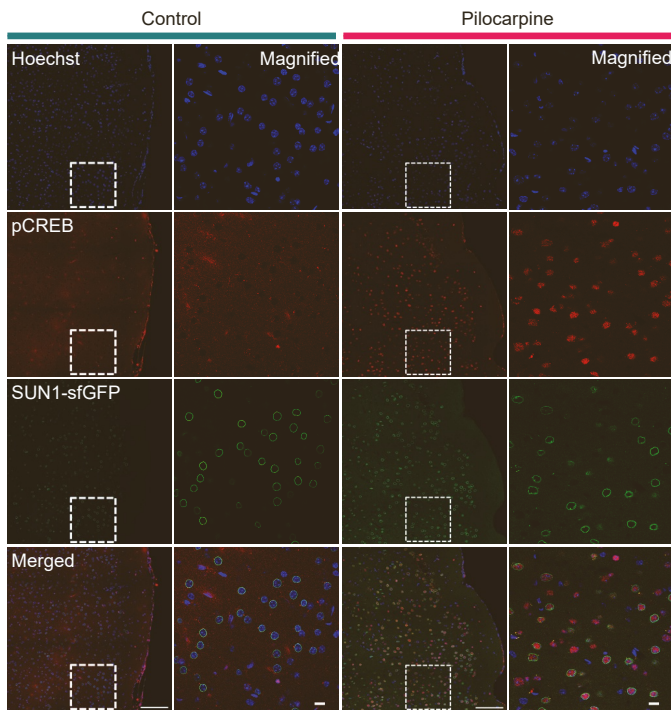
Figure S21: Coverage plots for DEGs (related to Figure 6A-C). Coverage plots for mock and seizure conditions for select genes showing differential expression at intron and exon levels.

SUPPLEMENTARY FIGURE

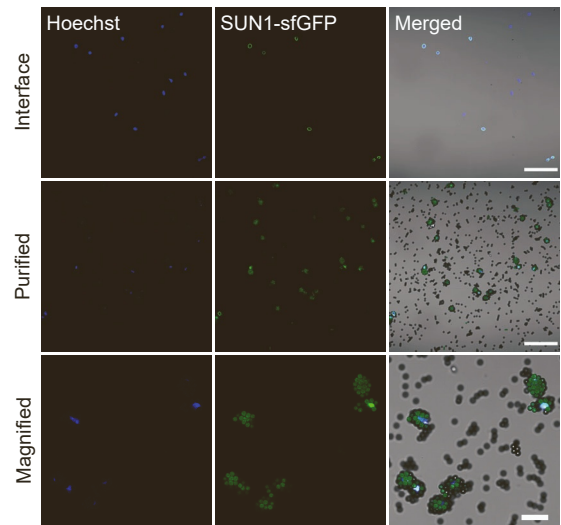
S1 CaMKII α -Cre:SUN1-sfGFP expression in excitatory neurons



S2 pCREB (S133) expression is elevated in the cortex



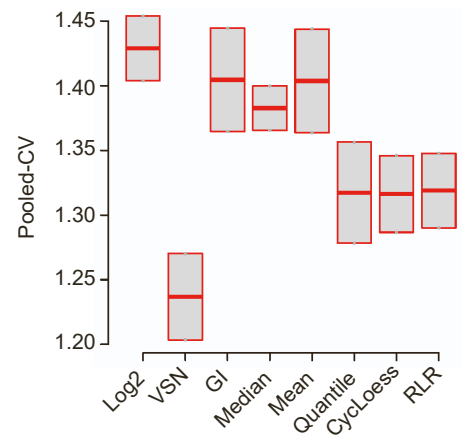
S3 INTACT isolation of nuclei at the interface stage



S4 INTACT nuclear purification efficiency

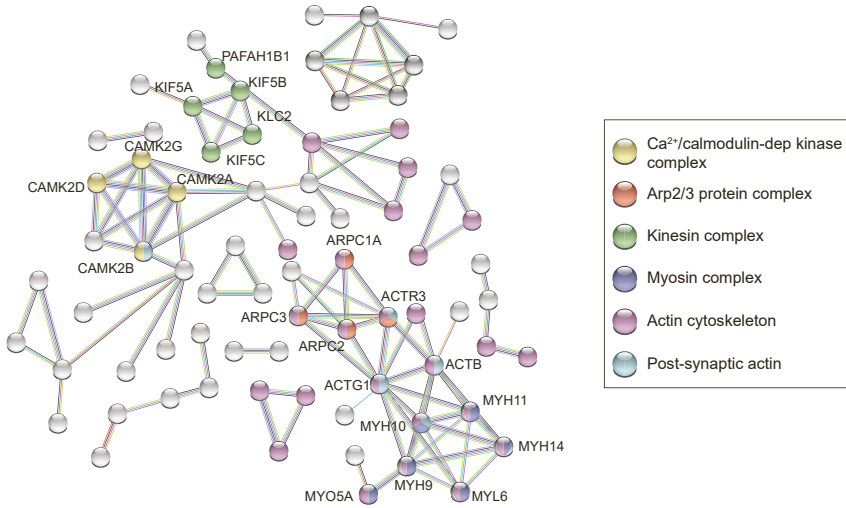
	Interface		Purified	
	GFP+ve (%)	Specificity (% GFP+ve)	No. of isolated nuclei per mouse ($\times 10^6$)	Yield (% interface)
Isolated nuclei (N=2)	43.05 \pm 2.85	100	4.43 \pm 0.1	78.95 \pm 8.15

S5 TMT6-labeled MS/MS VSN normalization

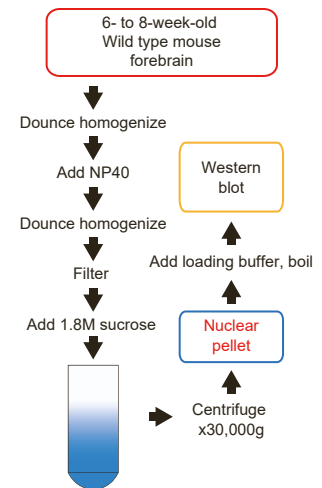


SUPPLEMENTARY FIGURE

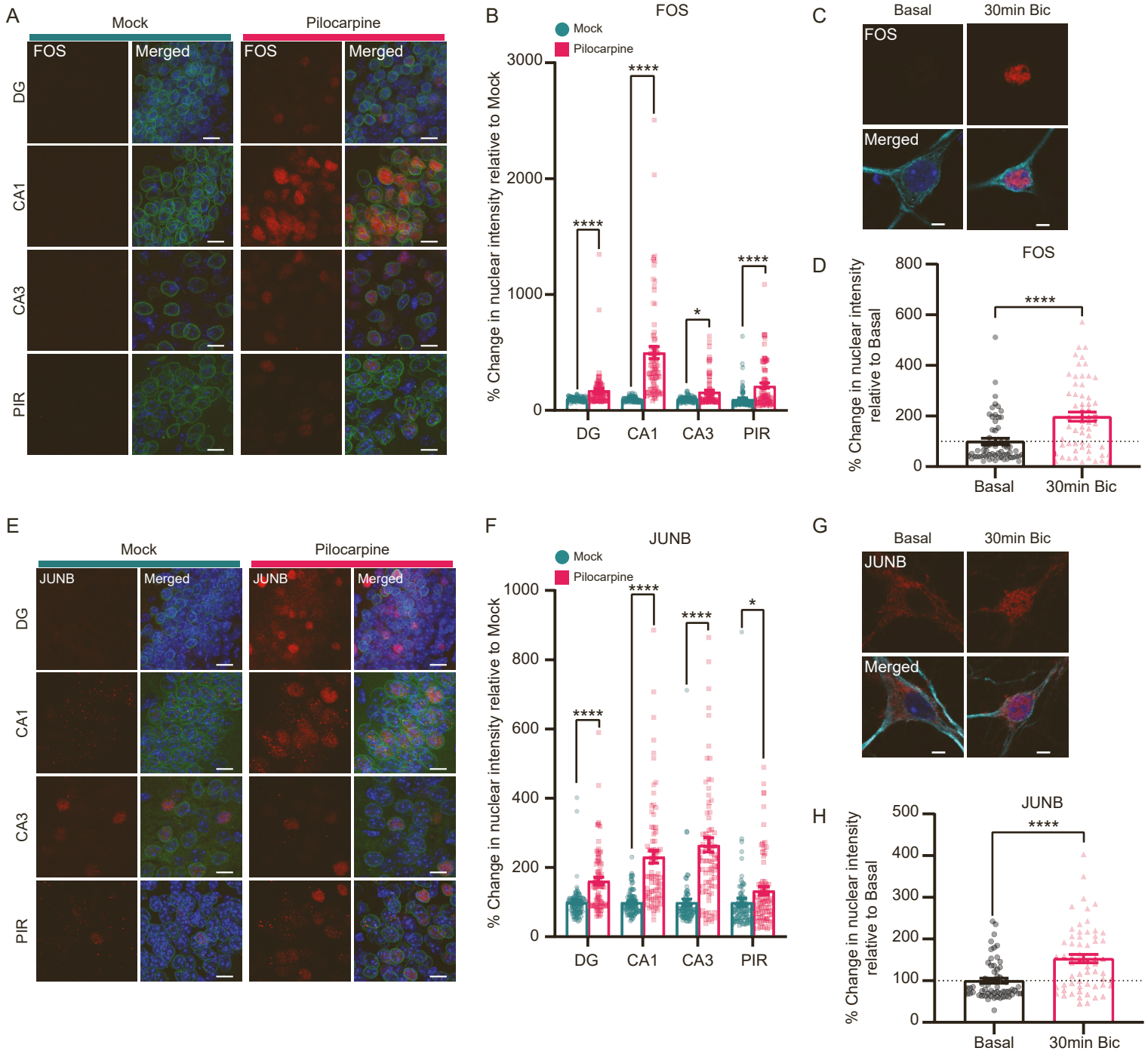
S6 STRING network of seizure-depleted nuclear proteins



S7 Flowchart for nuclear extraction



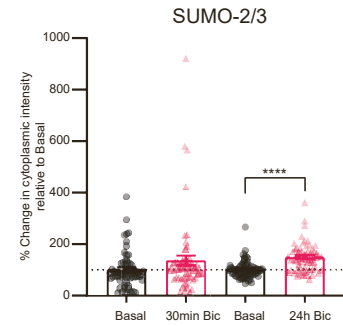
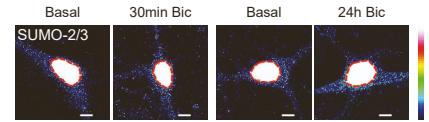
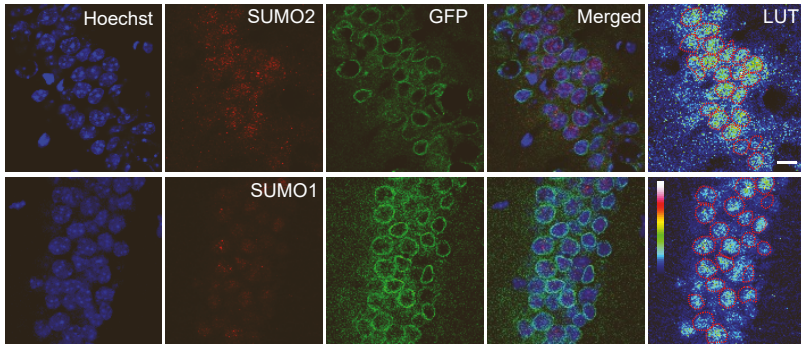
S8 AP1 complex expression during seizures in hippocampal neurons



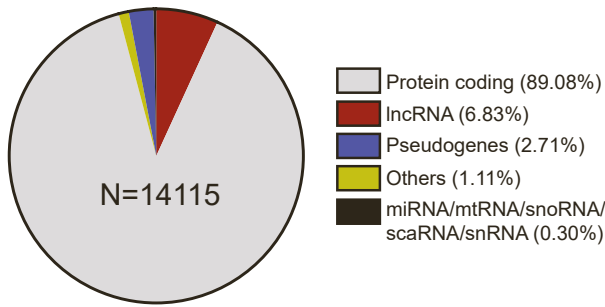
SUPPLEMENTARY FIGURE

S10 Cytoplasmic SUMO-2/3 after BIC stimulation

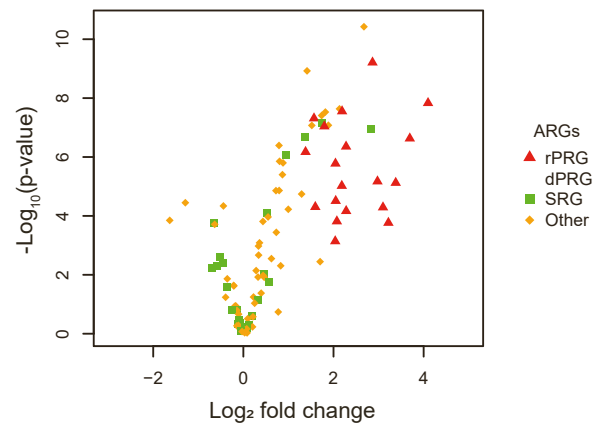
S9 Nuclear localization of SUMO-1 and SUMO-2/3 in neuronal nuclei



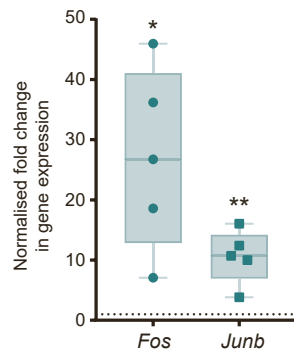
S11 Distribution of expressed transcript groups



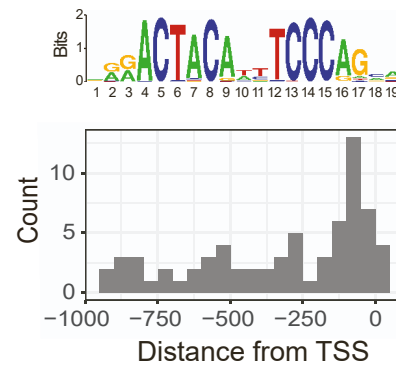
S12 Expression of known activity-regulated genes



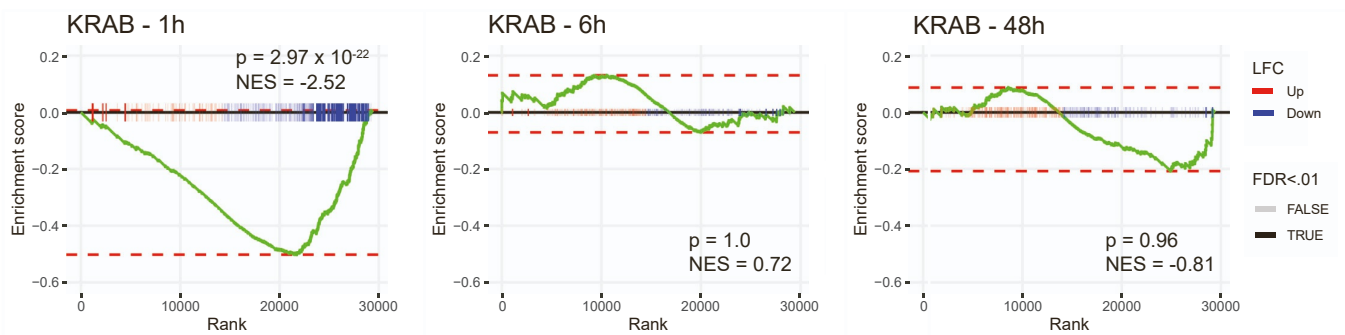
S13 Upregulation of *Fos* and *Junb* gene expression in seizing animals by qPCR



S14 THAP11 bipartite DNA binding motif

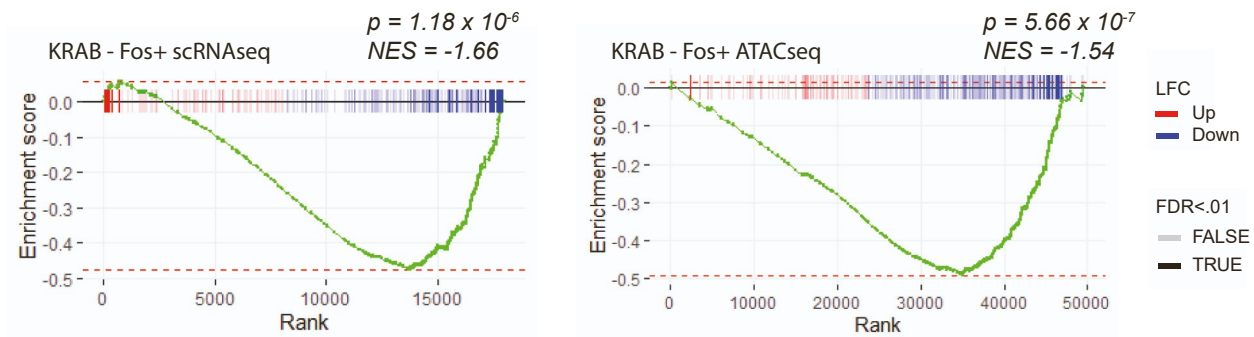


S15 Kainic acid-induced seizures downregulate KRAB-ZFP gene expression

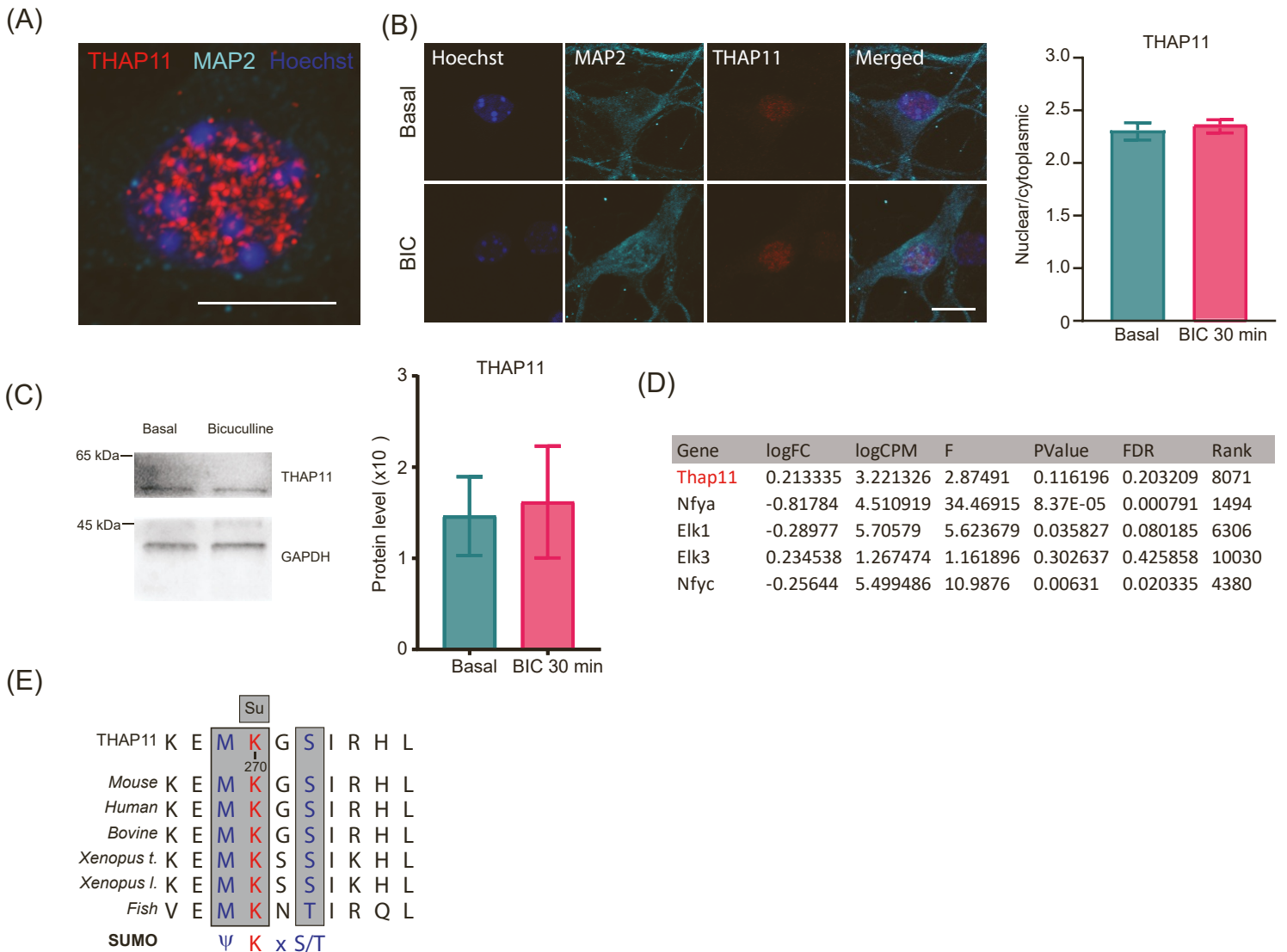


SUPPLEMENTARY FIGURE

S16 Exposure of rodents to novel environment drives activity-dependent suppression of KRAB-ZFPs

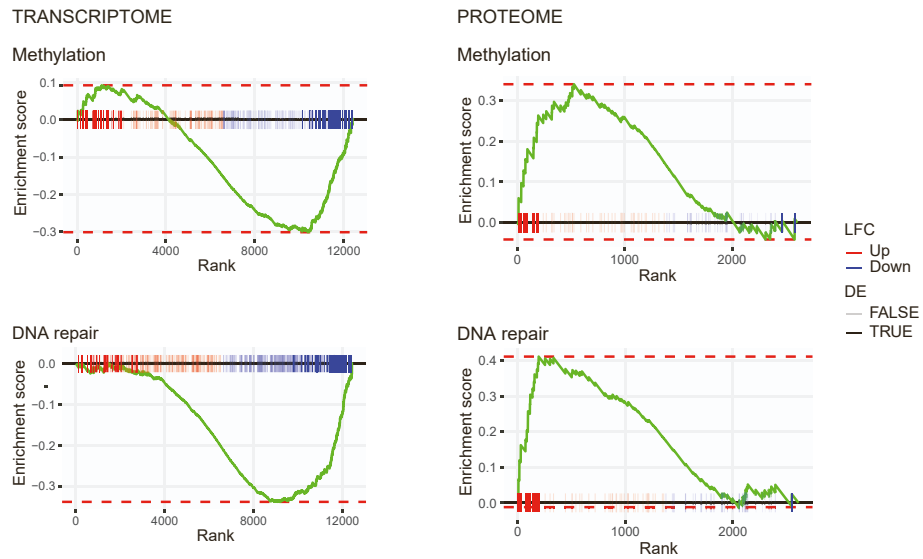


S17 THAP11 is localized in neuronal nuclei but the protein concentration and subcellular localization is not altered in the presence of bicuculline



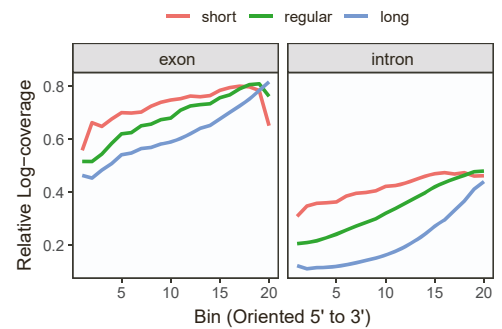
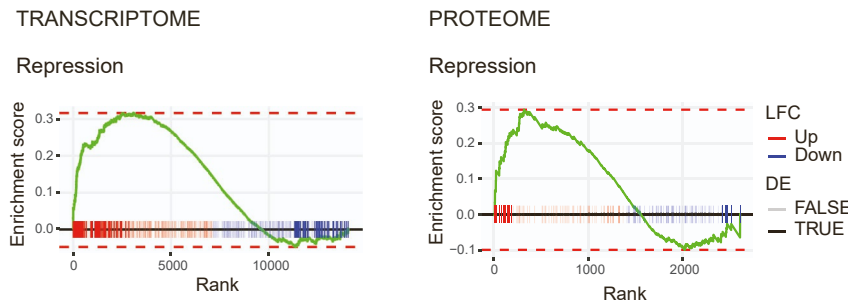
SUPPLEMENTARY FIGURE

S18 GSEA profiles of Methylation and DNA repair in nuclear proteome and transcriptome



S19 GSEA profiles of transcriptional repression in nuclear proteome and transcriptome

S20 Coverage of introns and exons across genebody for transcripts of varying lengths



S21 Representative examples of coverage profiles for different subpopulations of mock vs. pilocarpine DEGs

